Journal of Cosmology and Astroparticle Physics
An IOP and SISSA journal

Prospects for the Giant Metrewave Radio Telescope to observe radio waves from ultra high energy particles interacting with the Moon

Sukanta Panda[1], **Subhendra Mohanty**[2], **Janardhan Padmanabhan**[3,5] **and Oscar Stål**[4]

[1] Departamento de Fisica Teorica C-XI and Instituto de Fisica Teorica IFT-UAM/CSIC C-XVI, Universidad Autonoma de Madrid, Cantoblanco, E-28049 Madrid, Spain
[2] Physical Research Laboratory, Ahmedabad-380 009, India
[3] Instituto Nacional de Pesquisas Espaciais (INPE), Divisao de Astrofisica, Brazil
[4] High-Energy Physics, Department of Nuclear and Particle Physics, Uppsala University, PO Box 535, SE-751 21 Uppsala, Sweden
E-mail: sukanta@delta.ft.uam.es, mohanty@prl.res.in, jerry@das.inpe.br and oscar.stal@tsl.uu.se

Received 20 August 2007
Accepted 29 October 2007
Published 22 November 2007

Online at stacks.iop.org/JCAP/2007/i=11/a=022
doi:10.1088/1475-7516/2007/11/022

Abstract. Ultra high energy (UHE) particles of cosmic origin impact the lunar regolith and produce radio signals through the Askaryan effect, signals that can be detected by Earth based radio telescopes. We calculate the expected sensitivity for observation of such events at the Giant Metrewave Radio Telescope, both for UHE cosmic rays (CR) and UHE neutrino interactions. We find that for 30 days of observation time a significant number of detectable events are expected, above 10^{20} eV, for UHE CR or neutrino fluxes close to the current limits. Null detection over a period of 30 days will lower the experimental bounds by a magnitude competitive with both present and future experiments at the very highest energies.

Keywords: ultra high energy cosmic rays, ultra high energy photons and neutrinos

ArXiv ePrint: 0708.1683

[5] On Sabbatical leave from the Physical Research Laboratory, Ahmedabad-380 009, India.

1475-7516/07/11022+16$30.00

JCAP11(2007)022

Contents

1. Introduction

The study of cosmic rays with energies near and above the Greisen–Zatsepin–Kuzmin (GZK) cut-off $\sim 5 \times 10^{19}$ eV [1, 2] is of great interest in particle astrophysics. Above the GZK energy, proton interactions $p + \gamma_{\rm CMB} \rightarrow N\pi$ with cosmic microwave background (CMB) photons are possible. The universe in effect becomes opaque over Mpc scales. Checking the existence of this cut-off is therefore an important motivation for cosmic ray experiments like AUGER [3] and HIRES [4]. Complementing the cosmic ray experiments, a number of experiments perform direct searches for ultra high energy (UHE) neutrinos from the GZK pion decays ($\pi^+ \rightarrow \mu^+\nu_\mu \rightarrow e^+\nu_{\rm e}\bar{\nu}_\mu\nu_\mu$). The search for neutrinos above the GZK energy is also motivated in the context of grand unification theories (GUT) [5]. Relic 'X'-particles with ultra high mass $M_X \sim 10^{22}$ eV originating from the GUT phase transition in the early universe could be decaying in the present epoch. Thereby they would produce UHE neutrinos. A final example presenting a possibility for UHE neutrino production is the Z-burst process [6, 7]. In this scenario, the highest energy cosmic rays are produced following resonant interactions ($\nu\bar{\nu} \rightarrow Z^0$) of UHE neutrinos with the relic neutrino background. To explain the full cosmic ray spectrum, this would require a very high flux of neutrinos in the $E_\nu \sim 10^{22}$ regime to be present. Limits constraining the possible UHE neutrino flux from these processes exist, with the most stringent one to date being presented by the ANITA-lite experiment [8].

Among the various methods for detecting ultra high energy (UHE) particles, a promising technique utilizes the Askaryan effect [9, 10]. The Askaryan effect is most easily described as a two-stage process. In the first step, electromagnetic cascades in a dense medium, induced by UHE particle interactions, develop a negative charge excess. This excess is the result of secondary scattering processes and e^+e^- recombination in the material. Second, as soon as the charge imbalance has developed, it starts to radiate Čerenkov radiation. For wavelengths longer than the transverse length scale of the shower (of order 10 cm), the charge excess will radiate coherently. The output power P then scales with the number of shower particles N (or with the primary particle energy $E_{\rm P} \propto N$), as $P \propto N^2$. This is in contrast to the characteristic $P \propto N$ scaling for an incoherent process, such as optical Čerenkov emission. The observable result from the Askaryan effect is

therefore the generation of strong, coherent, pulses of low frequency Čerenkov radiation which we will discuss in more detail below.

In a series of accelerator experiments, the Askaryan mechanism has been confirmed to work in different media. Most important for our purposes, it was tested for silica sand specifically to mimic the conditions of the lunar material [11]. It was first proposed by Askaryan [9], and later by Dagkesamanskiĭ and Zheleznykh [12], that the radio transparent lunar regolith (the 10–20 m deep surface layer of the Moon, consisting mainly of fractured rock) would be an ideal target for use in studying such UHE particles. An additional advantage is the absence of an atmosphere which implies that electromagnetic showers in the lunar regolith are caused by the primary cosmic particles.

A number of attempts at observing cosmic ray induced radio waves from the Moon have since been carried out using ground based radio telescopes. The first experiment [13] used the 64 m diameter Parkes radio telescope in Australia to make coincidence measurements from two polarization channels. A 500 MHz band centred at 1.425 GHz was used after making appropriate corrections for the ionospheric delay between two sub-bands. The second was the Goldstone lunar ultra high energy neutrino experiment (GLUE) [14] that used two large telescopes of the JPL/NASA Deep Space Network in Goldstone (CA). A third experiment of this kind took place at Kalyazin Radio Astronomical Observatory, using again a single 64 m radio telescope [15]. None of these experiments, however, resulted in any detection of signals from UHE particles. Under the name NuMoon, there is one currently on-going search using the Westerbork synthesis radio telescope (WSRT) in the Netherlands [16]. For future experiments with increased sensitivity there are proposals [17]–[19] to study this effect with upcoming radio telescopes like the low frequency array (LOFAR) and the square kilometre array (SKA), or to use lunar orbiting artificial satellites carrying one or more radio antennas [20, 21].

In this paper we study in detail the possibility of detection of UHE CR and neutrino radio waves from the Moon with the Giant Metrewave Radio Telescope (GMRT) facility [22]. The GMRT comprises 30 fully steerable dishes spread over distances up to 25 km, each with a diameter of 45 m. Half of these antennas are distributed randomly over about 1 km^2 in a compact array while the rest are spread out in an approximate 'Y' configuration. The GMRT currently operates in eight frequency bands around 150, 235, 325, 610 and 1000–1450 MHz. The shortest baseline is 100 m while the longest one is 26 km. The telescope has an effective area of 30 000 m^2 for frequencies up to 325 MHz and 18 000 m^2 at the higher frequencies. The RMS sensitivity of the GMRT, using a 2 s integration time and a bandwidth of 32 MHz, is 0.3 mJy and 0.03 mJy at 325 MHz and 1.4 GHz respectively. With such high sensitivity, we expect a substantial improvement from previous experiments in the measurement of the Askaryan radio waves from the Moon.

2. Radio waves from cascades in the lunar regolith

High energy charged particles from UHE cosmic ray (CR) or UHE neutrino interactions in the lunar regolith will initiate a cascading shower with total energy E_s and typical length scale [19]

$$L(E_s) = 12.7 + \frac{2}{3}\log_{10}\frac{E_s}{10^{20}\ \mathrm{eV}} \quad (1)$$

in units of radiation length. For the lunar regolith with radiation length $X_0 = 22.1$ g cm^{-2} and density $\rho = 1.7$ g cm^{-3}, the shower length for a particle with energy $E = 10^{20}$ eV is therefore 1.7 m. Since the particles in the cascade travel at speeds very close to c, the duration of the shower is $L/c \simeq 5.67$ ns. The radio pulses of about 6 ns duration which are emitted from the shower can suffer time delay as they propagate to the telescope, first through scattering inside the lunar material, then at the lunar–vacuum interface. Since we primarily consider wavelengths $\lambda \sim 1$ m, we assume that most irregularities are of smaller size, and the effects of scattering are therefore neglected. The influence of radio wave scattering constitutes a systematic uncertainty in the estimated number of observable events, in particular at higher frequencies, since scattered radiation does not maintain the characteristic time structure of Askaryan emission [15]. A further time delay is caused to all pulses leaving the lunar regolith by dispersion as they propagate through the atmosphere of the Earth. The electrons in the ionosphere cause a time delay [18] of

$$t_{\rm d}(\nu) = 1.34 \times 10^{-7} \left(\frac{N_{\rm e}}{\rm m^{-2}}\right) \left(\frac{\rm Hz}{\nu}\right)^2 \tag{2}$$

seconds, where $N_{\rm e} = 10^{17}$ m^{-2} is the typical night-time column density of electrons. The dispersion of a radio signal of frequency ν and bandwidth $\Delta\nu$ at zenith is therefore

$$\Delta t_{\rm d} = 134 \text{ ns} \times \left(\frac{\Delta\nu}{40 \text{ MHz}}\right) \left(\frac{200 \text{ MHz}}{\nu}\right)^3. \tag{3}$$

One must thus look for Čerenkov radio pulses of about 100 ns duration from the Moon and use coherent de-dispersion to recover the broadband structure of the signals.

The intensity of radio waves on Earth from a shower in the lunar regolith with energy $E_{\rm s}$ emitting Čerenkov emission has been parametrized from simulations [19, 23, 24]. At an angle θ to the shower axis, for radiation frequency ν and bandwidth $\Delta\nu$, it is given by

$$F(E_{\rm s}, \theta, \nu) = 5.3 \times 10^5 \, f(E_{\rm s}, \theta) \left(\frac{E_{\rm s}}{\rm TeV}\right)^2 \times \left(\frac{1\,\rm m}{R}\right)^2 \left(\frac{\nu}{\nu_0[1 + (\nu/\nu_0)^{1.44}]}\right)^2 \frac{\Delta\nu}{100\,\rm MHz} \text{ Jy} \tag{4}$$

where R is the distance from the emission point on the Moon's surface to the telescope and $\nu_0 = 2.5$ GHz. Since the shower is not of infinite longitudinal extent, there is a non-trivial angular distribution $f(E_{\rm s}, \theta)$ around $\theta_{\rm C}$. The radiation intensity in a certain direction is dictated by the loss of coherence, which happens faster for frequencies closer to ν_0. The resulting angular distribution obtained from shower simulations is [19, 23, 24]

$$f(E_{\rm s}, \theta) = \left(\frac{\sin\theta}{\sin\theta_{\rm C}}\right)^2 \exp(-2Z^2), \tag{5}$$

with $Z = \sqrt{\kappa}(\cos\theta_{\rm C} - \cos\theta)$ and $\kappa(E_{\rm s}) = (\nu/\text{GHz})^2(70.4 + 3.4\ln(E_{\rm s}/\text{TeV}))$ for the lunar regolith. This radiation pattern is illustrated in figure 1. There we also show the commonly used Gaussian approximation where the forward-suppression factor $\sin^2\theta$ in (5) is ignored. For high frequencies, this approximation has no effect. For low frequencies, the difference at small angles only plays a role for showers nearly parallel to the surface normal, while the effect of changing the normalization near the Čerenkov angle is important also for

JCAP11(2007)022

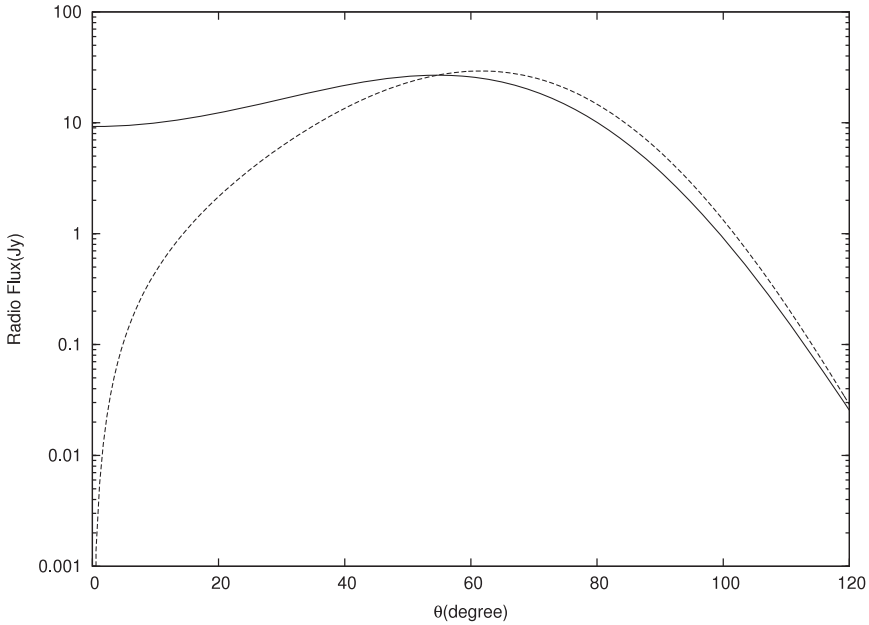

Figure 1. Radio flux at Earth from the centre of the Moon versus emission angle θ at $\nu = 150$ MHz and bandwidth $\Delta\nu = 40$ MHz for a shower initiated with $E_s = 10^{20}$ eV. The dashed line contains the complete dependence on θ in equation (5), whereas the full line shows the result of using the Gaussian approximation.

more horizontal showers. A measure of the effective angular spread Δ_C of the emission around the Čerenkov angle θ_C is given in terms of

$$\Delta_C = \sqrt{\frac{\ln(2)}{\kappa(E_s)}} \frac{1}{\sin\theta_C}. \tag{6}$$

For the example in figure 2 this becomes $\Delta_C \simeq 44°$. The Čerenkov radio waves are expected to be 100% linearly polarized [23]. Radio signals should therefore be observed with both the LCP and RCP modes. A simultaneous triggering of the LCP and RCP modes (with 50% of the total intensity in each mode) will be a good signature of the transient Čerenkov radio wave emission from UHE particles. In addition, the large number of GMRT dishes should allow pointing discrimination and spatial–temporal coincidence measurements to be used for signal identification and background rejection.

3. Aperture for cosmic ray and neutrino events at GMRT

For cosmic rays, which produce showers by hadronic processes, the shower energy E_s is equal to the energy of the primary particle. When instead the showers are produced by deep inelastic neutrino scattering off target nucleons, the fraction of the total energy which produces the hadronic showers is, on average, $E_s = 0.25E_P$ [25].

We model the lunar regolith as a homogeneous medium with dielectric permittivity $\epsilon = 3$, and hence refractive index $n = 1.73$. The Čerenkov angle is $\theta_C = 54.7°$. The radio waves are also absorbed in the regolith, which we take to have a frequency dependent

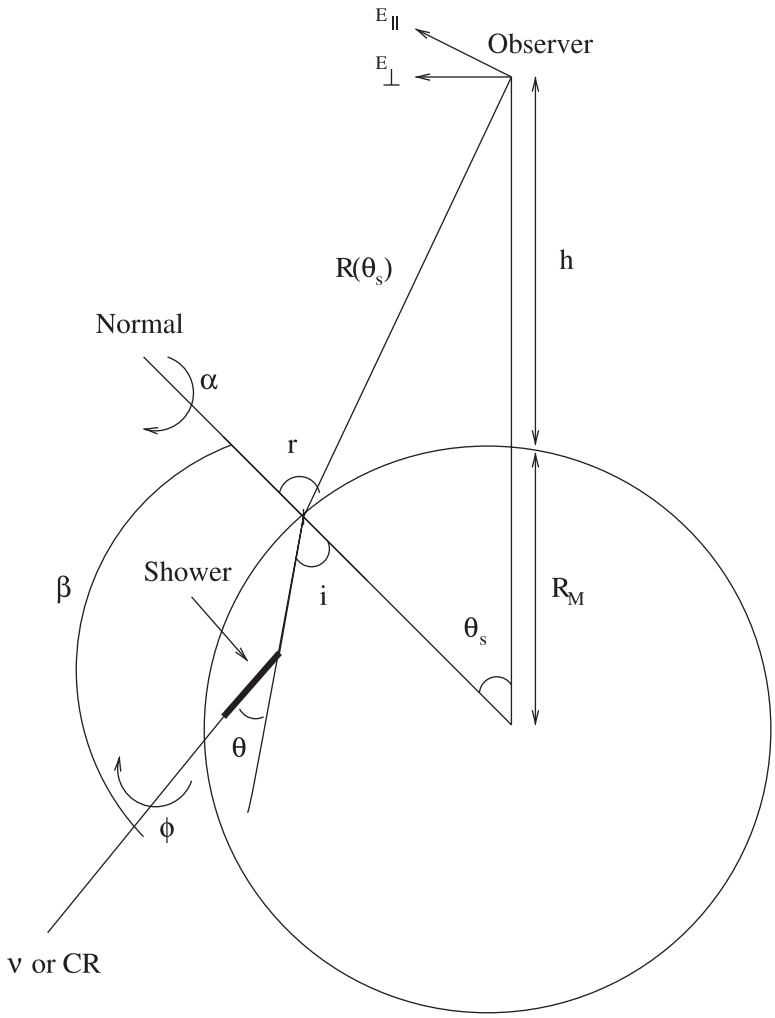

Figure 2. Geometry of an UHE CR or neutrino event which generates Čerenkov radiation of radio waves in the lunar regolith. The observer at Earth is located at a mean distance h from the lunar surface. The field components are oriented parallel ($E_{\|}$) and perpendicular ($E_{\perp}$) to the refraction plane.

attenuation length $\lambda_r = 9/(\nu/\mathrm{GHz})$ m [26]. This means that the attenuation length of radio waves is always much smaller than the mean free path of the neutrinos, conveniently parametrized as $\lambda_\nu = 670(1\,\mathrm{EeV}/E_\nu)^{0.363}$ km using the cross sections of [25]. As can be seen from this expression, the mean free path for an UHE neutrino is not sufficient for escaping the Moon. Most of the passing neutrinos will therefore interact in the material.

The threshold energy required for showers to be detectable is determined by the sensitivity of the radio telescope. To determine the sensitivity, we start from the expression for the background noise intensity

$$F_N = \frac{2k_B T_{sys}}{\sqrt{\delta t \Delta\nu} A_{eff}}, \tag{7}$$

where T_{sys} is the system temperature, k_B is Boltzmann's constant, δt the integration time, $\Delta\nu$ the bandwidth, and A_{eff} the effective area of the telescope. In Jansky

Table 1. GMRT parameters, sensitivity and threshold energy. F_N is the noise intensity of GMRT and $\mathcal{E}_N$ the corresponding electric field. The threshold energy in the last column is calculated with $\sigma = 25$.

ν (MHz)	T_{sys} (K)	$\Delta\nu$ (MHz)	F_N (Jy)	$\mathcal{E}_N$ (μV m^{-1} MHz^{-1})	$E_{th}(0)/\sqrt{\sigma}$ (eV)
150	482	40	44	0.0029	1.28×10^{20}
235	177	40	16	0.0017	5.04×10^{19}
325	108	40	10	0.0013	2.9×10^{19}
610	101	60	15	0.0014	1.68×10^{19}
1390	72	120	11	0.0008	5.6×10^{18}

(1 Jy $= 10^{-26}$ W m^{-2} Hz^{-1}) the noise intensity is given by

$$F_N = 2.76 \times 10^3 \frac{(T_{sys}/\mathrm{K})}{\sqrt{\delta t \Delta\nu}(A_{eff}/\mathrm{m}^2)}. \tag{8}$$

At GMRT, for frequencies 150, 235 and 325 MHz we use the effective area $A_{eff} = 30\,000$ m^2 while for the higher frequencies $A_{eff} = 18\,000$ m^2. The integration time $\delta t = 1/\Delta\nu$ for the bandwidth limited case. In table 1 we list the system temperatures at the different observation frequencies and the corresponding noise levels. The Moon will be filling the GMRT beam at 610 MHz and higher and since the full Moon has a background temperature of ∼230 K, T_{sys} will be dominated by this at higher frequencies. However, since this background temperature drops down significantly with the reducing phase of the Moon, column 2 in table 1 does not take this into account. Using equation (4), we can solve for E_s at the threshold required for measurement with the radio telescope (obtained for $\theta = \theta_C$ and $F = F_N$). If we take a required signal-to-noise ratio σ, the threshold shower energies E_{th} which can be measured at GMRT at the different observation frequencies are listed in table 1.

The radio waves produced below the lunar surface get attenuated while propagating to the surface and they get refracted at the surface before reaching the telescope. It is also possible that surface irregularities could lead to an increase of the effective angle over which UHE events can be detected [15]. Adopting a conservative approach, we use a flat lunar surface model with no enhancements due to surface slope. The transmission coefficients are different for the electric field polarization which is parallel and perpendicular to the lunar surface. It is therefore convenient to express the Čerenkov radiation intensity (4) in terms of the electric field magnitude $\mathcal{E}$ of the radio waves. The conversion is

$$\frac{F}{\mathrm{Jy}} = \frac{10^7}{24\pi} \left(\frac{\mathcal{E}}{\mu\mathrm{V/m/MHz}}\right)^2 \frac{\Delta\nu}{\mathrm{MHz}}. \tag{9}$$

Using this conversion we also list the threshold electric fields measurable at GMRT in table 1. If attenuation is factored in separately, the quantity $R\mathcal{E}$ remains a constant between the point of emission and the point of refraction at the surface:

$$R\mathcal{E} = 0.2\,\mathrm{e}^{-Z^2} \left(\frac{E_s}{\mathrm{TeV}}\right) \times \left(\frac{\nu}{\nu_0[1 + (\nu/\nu_0)^{1.44}]}\right) \frac{\mu\mathrm{V}}{\mathrm{MHz}}. \tag{10}$$

At the surface, there is partial reflection, which changes the intensity of the outgoing electric field. For a purely refracted pulse, the electric field observed at the telescope relates to the incident electric fields through the Fresnel relations

$$T_\perp = \frac{R\mathcal{E}_\perp}{(R\mathcal{E}_\perp)_{\rm inc}} = \frac{2\cos r}{n\cos i + \cos r}$$
$$T_\parallel = \frac{R\mathcal{E}_\parallel}{(R\mathcal{E}_\parallel)_{\rm inc}} = \frac{2\cos r}{n\cos r + \cos i} \tag{11}$$

where the angles of incidence i and refraction r are related by Snell's law. In these relations, parallel and perpendicular field components refer to their orientation with respect to the plane of refraction. Using the notation of figure 2, the refraction angle r is fixed by the polar angle $\theta_{\rm s}$ through the geometrical condition

$$\sin(r) = \frac{\sin(\theta_{\rm s})(R_{\rm M}+h)}{R(\theta_{\rm s})}. \tag{12}$$

Here $R(\theta_{\rm s}) = [R_{\rm M}^2 + (R_{\rm M}+h)^2 - 2(R_{\rm M}+h)R_{\rm M}\cos\theta_{\rm s}]^{1/2}$ is the distance between the detector and the point of refraction on the lunar surface, and $h = 384\,000$ km is the average Earth–Moon distance. Putting everything together, the parallel component of the electric field at the telescope on Earth is given by

$$\mathcal{E}_\parallel = \frac{1}{R(\theta_{\rm s})} T_\parallel(\theta_{\rm s})(R\mathcal{E})_{\rm inc}, \tag{13}$$

where $(R\mathcal{E})_{\rm inc}$ is given by (10) as a function of θ and $E_{\rm s}$. The dependence on the polar angle $\theta_{\rm s}$ of the radio flux on Earth is shown in figure 3.

Evaluating $(R\mathcal{E})_{\rm inc}$ at $\theta = \theta_{\rm C}$ and equating $\mathcal{E}_\parallel$ with the threshold field $\mathcal{E}_{\rm th}$ which can be measured with the telescope, we obtain the threshold energy $E_{\rm th}$ as a function of the polar angle $\theta_{\rm s}$. Figure 4 illustrates that for observing the radio waves from the limb of the Moon ($\theta_{\rm s} \to \pi/2$ for $h \gg R_{\rm M}$), one has to have a higher threshold energy of the shower owing to the fact that the transmission coefficients $T_\perp$ and $T_\parallel$ vanish when $r \to \pi/2$. If h was not large compared to $R_{\rm M}$, e.g. for a detector aboard a satellite orbiting the Moon, only a small disc around the centre of the Moon would be visible.

By equating the signal $\mathcal{E}_\parallel = \sqrt{\sigma}\mathcal{E}_N$ at the Čerenkov angle we determine the threshold $E_{\rm th}(\theta_{\rm s} = 0)$ at different frequencies and bandwidths. The values so obtained are listed in table 1.

The event rate that would be expected at the telescope can be related to an isotropic flux Φ of UHE particles on the Moon through

$$\frac{{\rm d}N_i}{{\rm d}t} = \int \frac{{\rm d}\Phi_i}{{\rm d}E} A_i(E){\rm d}E, \tag{14}$$

where $i = \{{\rm CR}, \nu\}$ denote the type of primary particle and $A_i(E)$ is an aperture function corresponding to the effective detector area. We will differentiate between neutrinos, which have a large mean free path and therefore can penetrate the interior of the Moon before

JCAP11(2007)022

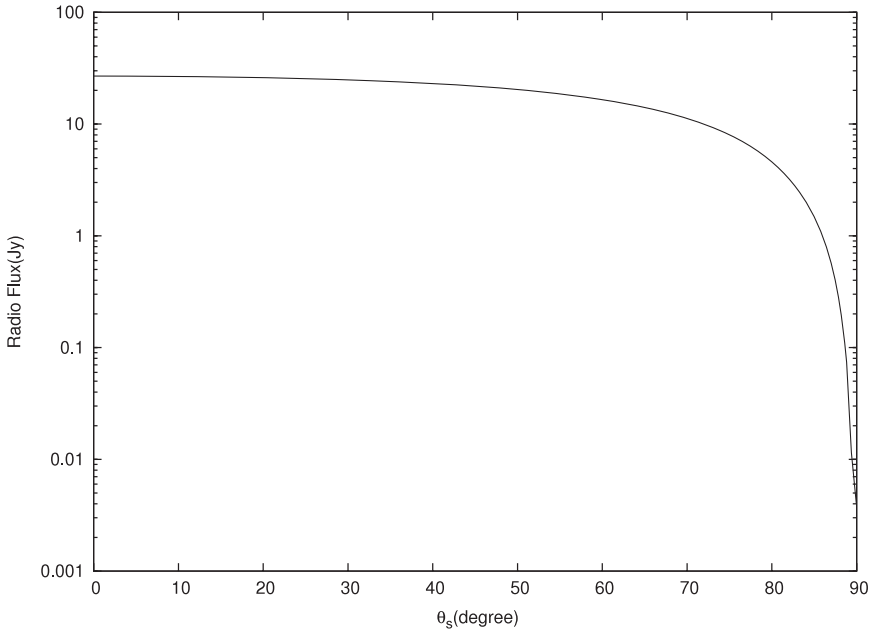

Figure 3. Radio flux at Earth versus the lunar polar angle θ_s for $\theta = \theta_c$. The frequency $\nu = 150$ MHz, and the bandwidth $\Delta\nu = 40$ MHz. The shower was initiated with an energy $E_s = 10^{20}$ eV.

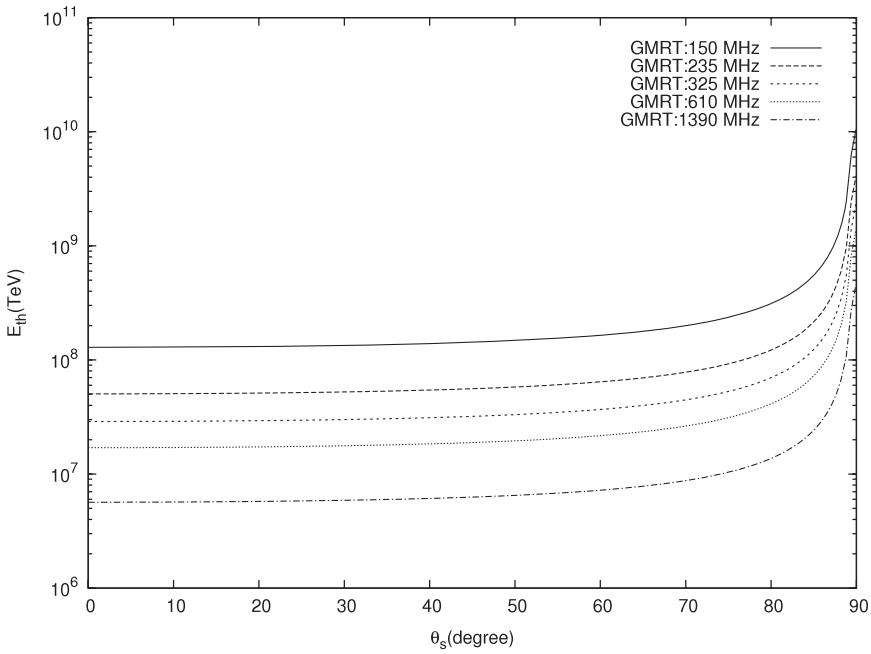

Figure 4. Shower threshold energy as a function of the polar angle θ_s on the Moon, for a detection signal-to-noise ratio $\sigma = 25$.

producing the Čerenkov radio waves, and the strongly interacting cosmic rays (referred to by the subscript CR) which can penetrate only small distances below the surface of the Moon. The aperture can be further decomposed into an angular aperture $\Delta\Omega_i(E, \theta_s)$ and

a geometric area factor for the Moon

$$A_i(E) = 2\pi R_M^2 \int \Delta\Omega_i(E, \theta_s) \mathrm{d}\cos\theta_s \tag{15}$$

with $R_M = 1760$ km. To evaluate the aperture, we use the analytical methods described in [20]. Using $\Theta(x)$ to denote the Heaviside (step) function, the angular aperture for the case of cosmic rays is given by

$$\Delta\Omega_{CR}(E, \theta_s) = \int \cos\beta \Theta[\mathcal{E}(E, \theta_s) - \mathcal{E}_{th}] \times \Theta(\cos\beta) \mathrm{d}\alpha \, \mathrm{d}\cos\beta, \tag{16}$$

where β and α are the polar and azimuthal coordinates of the ray normal to the Moon's surface in a system where the shower direction defines the z axis. The full geometry and the different angles are described in figure 1. Using the Gaussian approximation for the radiation pattern, the angular aperture for cosmic rays is obtained by directly integrating over the shower coordinates (θ, ϕ):

$$\Delta\Omega_{CR} = 2 \int_{1/n-D}^{\sin(i)} \mathrm{d}\cos\theta \int_0^{\phi_m} \mathrm{d}\phi [\sin(\theta)\sin(i)\cos(\phi) - \cos(\theta)\cos(i)]. \tag{17}$$

Here $\cos(\phi_m) = \cos(i)\cos(\theta)/\sin(i)\sin(\theta)$, and in the lower integration limit $D = \sqrt{(1/\kappa)\ln(E/E_{th})}$. This takes into account all directions with sufficiently strong radio emission. After performing this integration, the expression for the angular aperture reduces to

$$\Delta\Omega_{CR} = \cos^{-1}\left(\frac{\cos\theta_{max}}{\sin i}\right) - \sin(\theta_{max})\Big[\sin(\theta_{max})\cos(i)\phi_{max} + \cos(\theta_{max})\sin(i)\sin(\phi_{max})\Big], \tag{18}$$

where $\cos(\theta_{max}) = 1/n - D$ and $\cos(\phi_{max}) = \cos(i)\cos(\theta_{max})/\sin(i)\sin(\theta_{max})$. The total aperture for cosmic rays is obtained by substituting (18) in (15) and integrating over the polar angle θ_s.

When the UHE primary is instead a neutrino, it can produce showers deep below the surface of the Moon and there will be considerable attenuation of the radio waves which travel distances longer than λ_r below the surface. For the neutrino induced showers, the aperture is defined in the same way as for the CR, but the angular aperture is now given [20] by

$$\Delta\Omega_\nu(E, \theta_s) = \int \frac{\mathrm{d}z}{\lambda_\nu} \int \Theta\{\mathcal{E}(E, \theta_s, \theta)\exp[-z/(2\lambda_r\cos i)] - \mathcal{E}_{th}\} \times \exp[-L(z, \beta)/\lambda_\nu] \times \mathrm{d}\alpha \, \mathrm{d}\cos\beta, \tag{19}$$

where $L(z, \beta)$ is the distance the neutrino travels inside the material to reach the interaction point at a distance z below the surface. In performing this integration we allow z to go below the known depth of the regolith. The aperture can therefore pick up contributions from sufficiently strong signals coming from deep showers, especially for the lower frequencies. Numerically we find for the worst case (when $\nu = 150$ MHz), that imposing a sharp cut-off at a depth of 20 m would reduce the aperture by nearly an order of magnitude, similarly to what was discussed in [19].

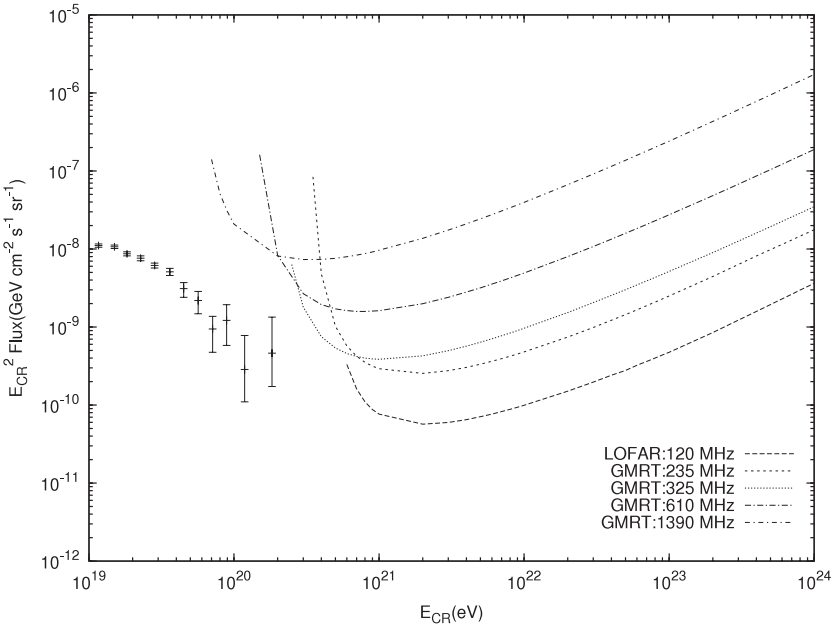

Figure 5. Model independent limits on UHE CR flux at different observation frequencies for 100 h of observation time with GMRT. The curve labelled LOFAR was obtained using the method of calculation presented in this paper, taking the LOFAR parameters of [19] as input. The same observation time was used. Auger data points on the CR flux from [28] are shown for comparison.

It has been observed [20], that if the absorption length of radio waves λ_r is much smaller than the neutrino mean free path λ_ν (which is indeed the case here) then equation (19) reduces approximately to

$$\Delta\Omega_\nu(E,\theta_s) = \int \frac{2\lambda_r \cos(i)}{\lambda_\nu} \ln(\mathcal{E}(E)/\mathcal{E}_{th})\Theta[\mathcal{E}(E,\theta_s,\theta) - \mathcal{E}_{th}] \times d\alpha\, d\cos\beta. \quad (20)$$

As for the cosmic rays, the total aperture is obtained by substituting (19) into (15) and integrating over the polar angle θ_s.

To estimate the sensitivity of GMRT to cosmic ray and neutrino events we have evaluated the angular apertures by employing this technique and performing numerical integrations for the different parameters given in table 1. In the next section we will discuss these results further in the context of prospective flux limits.

4. Limits on the flux of cosmic rays and neutrinos

Should no events be observed at GMRT during observation over a time T, an upper limit can be established on sufficiently smooth UHE CR and neutrino fluxes at the Moon. The conventional model independent limit [27] is given by

$$E_i^2 \frac{d\Phi_i}{dE_\nu} \leq s_{up} \frac{E_i}{A_i(E_s = y_i E_i)T}, \quad (21)$$

where still $i = \{\nu, CR\}$, $y_{CR} = 1$ and $y_\nu = 0.25$. The Poisson factor $s_{up} = 2.3$ for a limit at 90% confidence level. The limits on the flux of UHE CR that could be established for

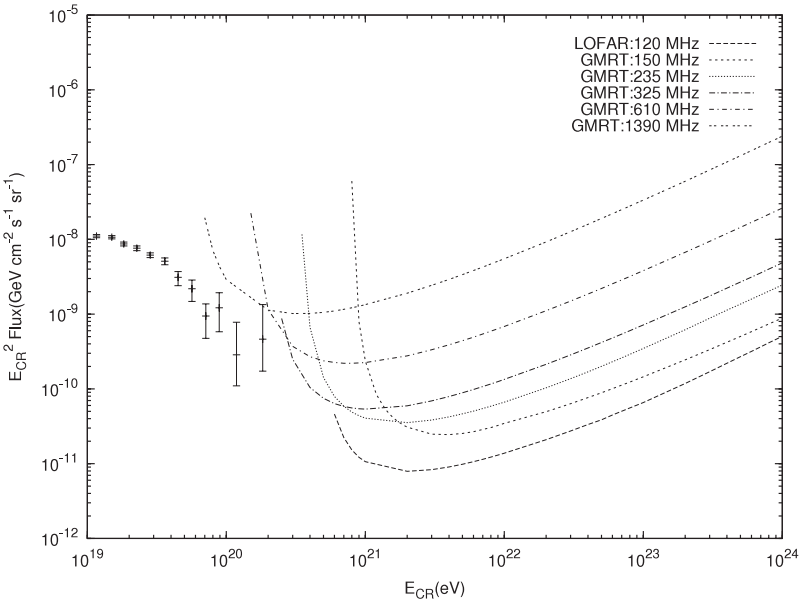

Figure 6. Model independent limits on UHE CR flux at different observation frequencies for 30 days of observation time with GMRT. The LOFAR curve was calculated as above, rescaled to $T = 30$ days. The Auger data are the same as above.

100 h and 30 days of observation time at GMRT are shown in figures 5 and 6 respectively. We also show the results of carrying through our calculations for the LOFAR parameters given in [19]. When compared to the LOFAR Monte Carlo simulation results, the two methods of calculation agree within a factor of two over the full energy range. This is an acceptable discrepancy in level with known uncertainties from e.g. the regolith depth. A residual difference of ∼30% is also expected since we used the Gaussian approximation. The limit we obtain for the LOFAR parameters is less stringent than the one published, so in this respect our result constitutes a conservative estimate. From comparing the limits for different frequencies, it can be seen that low frequency observations give stricter limits on the flux at the expense of a higher threshold. This is due to the well-known increase in the aperture [19] from radiation spreading at lower frequencies. The figures also show the Auger data [28] on UHE cosmic rays. Although the extrapolation to higher energies is highly uncertain, the GMRT would most probably be sensitive to a post-GZK proton flux.

Similarly for the UHE neutrinos, prospective limits on their flux for $T = 100$ h and $T = 30$ days are shown in figures 7 and 8. Also here we show a calculation for the LOFAR parameters, again in quantitative agreement with previous results. Since many radio experiments exist for UHE neutrino detection, we have compiled a comparison in figure 9. This figure contains, in addition to the GMRT results for $\nu = 150$ MHz with two different observation times, the already existing limits from RICE [29], GLUE [14], FORTE [27] and ANITA-lite [8]. Also we have indicated the prospective future limits that have been calculated for ANITA [8], LOFAR [19] or LORD [20].

5. Summary and conclusions

We have calculated the potential for GMRT to detect UHE cosmic rays and neutrinos through their radio wave emission produced when showering in the lunar regolith.

JCAP11(2007)022

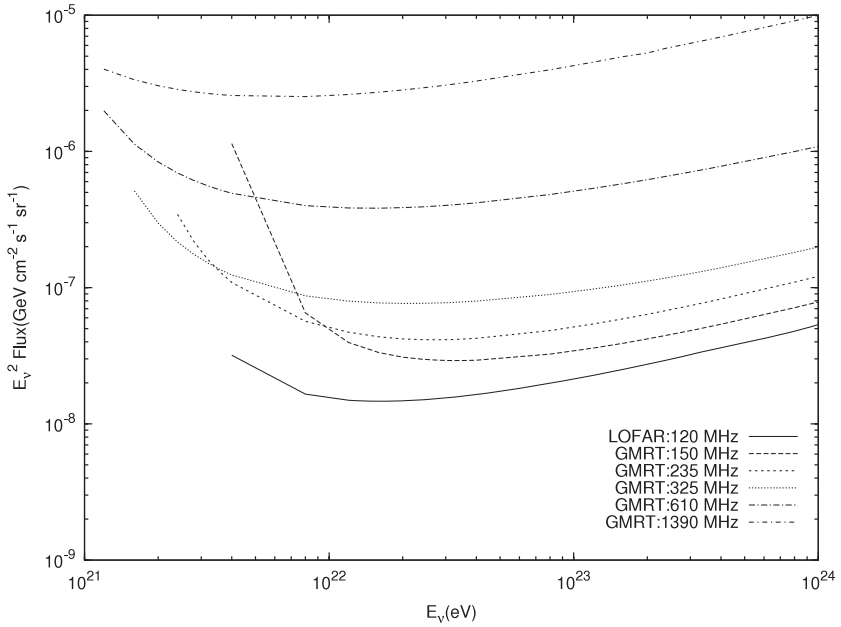

Figure 7. Model independent limits on UHE neutrino flux at different frequencies for 100 h of observation time with GMRT. The curve labelled LOFAR was obtained using the method of calculation presented in this paper, taking the LOFAR parameters of [19] as input. The same observation time was used.

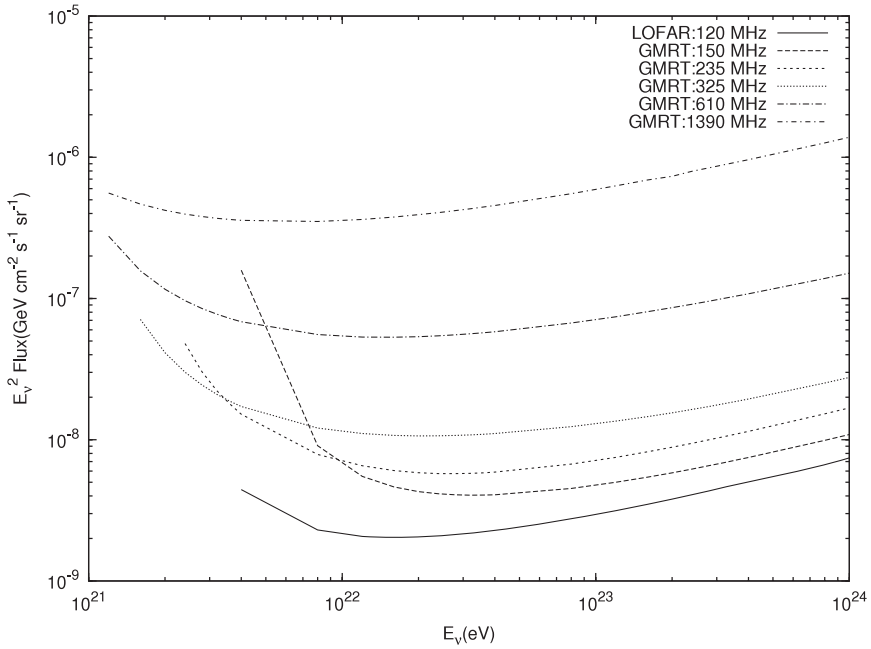

Figure 8. Mode independent limits on UHE neutrino flux at different frequencies for 30 days of observation time with GMRT. The LOFAR curve was calculated as above, rescaled to $T = 30$ days.

Our results indicate that GMRT could be competitive with future experiments in the $E \gtrsim 10^{20}$ eV range. If one assumes that the CR spectrum continues beyond the

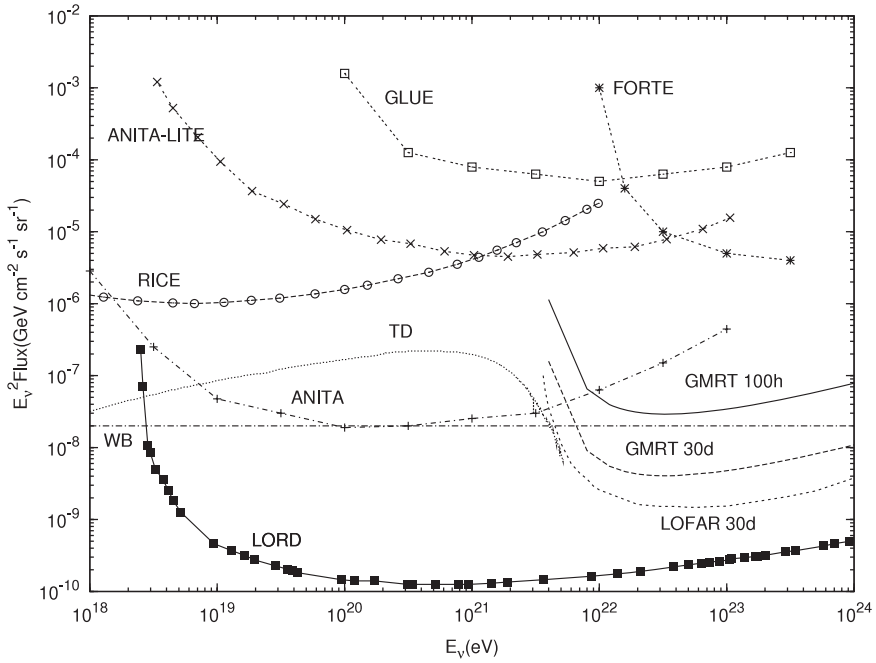

Figure 9. Prospective flux limits on UHE neutrinos from GMRT shown for effective exposure times of 100 hours and 30 days. The current best limits from radio experiments ANITA-lite [8], GLUE [14], FORTE [27], and RICE [29] are shown. For comparison the expected limits from future experiments ANITA [8], LOFAR [19] and LORD [20] are also included. The WB line indicates the theoretical upper limit of Waxman and Bahcall [30] on the cosmogenic neutrino flux. TD refers to the topological defect model with $M_X = 2 \times 10^{22}$ eV described in [31].

JCAP11(2007)022

GZK limit with unchanged energy dependence, observation of these particles with the GMRT should indeed be possible. For UHE neutrinos there exists a theoretical upper bound on the flux from cosmogenic sources, as given by Waxman and Bahcall [30]: $E_\nu^2 \Phi_\nu < 2 \times 10^{-8}$ GeV cm^{-2} s^{-1} sr^{-1}. The GMRT could, using a mere 30 days of observation time, probe fluxes a factor of five smaller. As a benchmark scenario, we indicate in figure 9 the predicted flux from one topological defect (TD) model [31] where the mass scale resides around 10^{22} eV.

It is notable that the GMRT (for the low frequencies) has only a somewhat higher threshold, and slightly worse sensitivity for this type of experiment, than the LOFAR telescope will have. This clearly points to the interesting potential of utilizing the GMRT for UHE particle searches in the near future. It is worthwhile to mention here that GMRT can also measure the polarization of radio waves. Hence from polarization study the plane of incidence of the original particle can be found. The results that we have presented here obviously depend on to what extent the experimental realizations of these measurements are possible at the GMRT facility. We therefore foresee a future analysis taking more thoroughly into account the requirements on the technical infrastructure and the experimental techniques for signal identification and background discrimination.

Acknowledgments

The authors thank Gunnar Ingelman for reading the manuscript, and for providing insightful comments and suggestions. We also thank Olaf Scholten for useful communication. The work of SP is supported by Ministerio de Educacion y Ciencia, Spain under Proyecto Nacional FPA2006-01105, and also by the Comunidad de Madrid under Proyecto HEPHACOS, Ayuda de I+D S-0505/ESP-0346. JP would like to acknowledge support under FAPESP project number 2006/56274-8.

References

[1] Greisen K, *End to the cosmic-ray spectrum?*, 1966 *Phys. Rev. Lett.* **16** 748 [SPIRES]
[2] Zatsepin G and Kuzmin V, *Upper limit of the spectrum of cosmic rays*, 1966 *JETP Lett.* **4** 78
[3] Yamamoto T (Pierre Auger Collaboration), *The UHECR spectrum measured at the Pierre Auger Observatory and its astrophysical implications*, 2007 *Preprint* 0707.2638 [astro-ph]
[4] Abbasi R *et al* (HiRes Collaboration), *Observation of the GZK cutoff by the HiRes experiment*, 2007 *Preprint* astro-ph/0703099
[5] Bhattacharjee P, Hill C T and Schramm D N, *Grand unified theories, topological defects and ultra high-energy cosmic rays*, 1992 *Phys. Rev. Lett.* **69** 567 [SPIRES]
[6] Fargion D, Mele B and Salis A, *Ultra high energy neutrino scattering onto relic light neutrinos in galactic halo as a possible source of highest energy extragalactic cosmic rays*, 1999 *Astrophys. J.* **517** 725 [SPIRES] [astro-ph/9710029]
[7] Weiler T J, *Cosmic ray neutrino annihilation on relic neutrinos revisited: a mechanism for generating air showers above the Greisen–Zatsepin–Kuzmin cut-off*, 1999 *Astropart. Phys.* **11** 303 [SPIRES] [hep-ph/9710431]
[8] Barwick S W *et al* (ANITA Collaboration), *Constraints on cosmic neutrino fluxes from the ANITA experiment*, 2006 *Phys. Rev. Lett.* **96** 171101 [SPIRES] [astro-ph/0512265]
[9] Askaryan G A, *Excess negative charge of an electron–photon shower and its coherent radio emission*, 1962 *Sov. Phys. JETP* **14** 441 [SPIRES]
[10] Askaryan G A, *Coherent radio emission form cosmic showers in air and in dense media*, 1965 *Sov. Phys. JETP* **21** 658 [SPIRES]
[11] Saltzberg D *et al*, *Observation of the Askaryan effect: coherent microwave Cherenkov emission from charge asymmetry in high-energy particle cascades*, 2001 *Phys. Rev. Lett.* **86** 2802 [SPIRES]
[12] Dagkesamanskiĭ R D and Zheleznykh I M, *Radio-astronomy method for detecting neutrinos and other elementary particles at superhigh energies*, 1989 *Sov. Phys. JETP* **50** 233 [SPIRES]
[13] James C W, Crocker R M, Ekers R D, Hankins T H, O'Sullivan J D and Protheroe R J, *Limit on UHE neutrino flux from the Parkes lunar radio Cherenkov experiment*, 2007 *Mon. Not. R. Astron. Soc.* **379** 1037 [astro-ph/0702619]
[14] Gorham P W *et al* (GLUE Collaboration), *Experimental limit on the cosmic diffuse ultra high energy neutrino flux*, 2004 *Phys. Rev. Lett.* **93** 041101 [SPIRES]
[15] Beresnyak A R, Dagkesamansky R D, Kovalenko A V, Oreshko V V and Zheleznykh I M, *Limits on the flux of ultra high-energy neutrinos from radio astronomical observations*, 2005 *Astron. Rep.* **49** 127
[16] Scholten O, 2006 private communication
[17] Alvarez-Muniz J and Zas E, *Prospects for radio detection of extremely high energy cosmic rays and neutrinos in the Moon*, 2001 *AIP Conf. Proc.* **579** 128 [astro-ph/0102173]
[18] Falcke H, Gorham P and Protheroe R J, *Prospects for radio detection of ultra-high energy cosmic rays and neutrinos*, 2004 *New Astron. Rev.* **48** 1487 [astro-ph/0409229]
[19] Scholten O, Bacelar J, Braun R, de Bruyn A G, Falcke H, Stappers B and Strom R G, *Optimal radio window for the detection of ultra-high-energy cosmic rays and neutrinos off the moon*, 2006 *Astropart. Phys.* **26** 219 [SPIRES] [astro-ph/0508580]
[20] Gusev G A *et al* (LORD Collaboration), *Detection of ultra high-energy cosmic rays and neutrinos by radio method using artificial lunar satellites*, 2006 *Cosmic Res.* **44** 19
[21] Stål O, Bergman J, Thide B, Daldorff L K S and Ingelman G, *Prospects for lunar satellite detection of radio pulses from ultra high energy neutrinos interacting with the moon*, 2007 *Phys. Rev. Lett.* **98** 071103 [SPIRES] [astro-ph/0604199]
[22] GMRT website http://www.gmrt.ncra.tifr.res.in

[23] Zas E, Halzen F and Stanev T, *Electromagnetic pulses from high-energy showers: implications for neutrino detection*, 1992 *Phys. Rev.* D **45** 362 [SPIRES]
[24] Alvarez-Muniz J, Marques E, Vazquez R A and Zas E, *Coherent radio pulses from showers in different media: a unified parameterization*, 2006 *Phys. Rev.* D **74** 023007 [SPIRES] [astro-ph/0512337]
[25] Gandhi R, Quigg C, Reno M H and Sarcevic I, *Neutrino interactions at ultra high energies*, 1998 *Phys. Rev.* D **58** 093009 [SPIRES] [hep-ph/9807264]
[26] Olhoeft G R and Strangway D W, *Dielectric properties of the first 100 meters of the moon*, 1975 *Earth Planet. Sci. Lett.* **24** 394
[27] Lehtinen N G, Gorham P W, Jacobson A R and Roussel-Dupre R A, *FORTE satellite constraints on ultra-high energy cosmic particle fluxes*, 2004 *Phys. Rev.* D **69** 013008 [SPIRES] [astro-ph/0309656]
[28] Semikoz D V (Pierre Auger Collaboration), *Constraints on top-down models for the origin of UHECRs from the Pierre Auger observatory data*, 2007 *Preprint* 0706.2960 [astro-ph]
[29] Kravchenko I *et al* (RICE Collaboration), *RICE limits on the diffuse ultra-high energy neutrino flux*, 2006 *Phys. Rev.* D **73** 082002 [SPIRES] [astro-ph/0601148]
[30] Waxman E and Bahcall J N, *High energy neutrinos from astrophysical sources: an upper bound*, 1999 *Phys. Rev.* D **59** 023002 [SPIRES] [hep-ph/9807282]
[31] Semikoz D V and Sigl G, *Ultra-high energy neutrino fluxes: new constraints and implications*, 2004 *J. Cosmol. Astropart. Phys.* JCAP04(2004)003 [SPIRES] [hep-ph/0309328]

JCAP11(2007)022